Differentiating between *ortho*- and *para*-Quinone Surface Groups on Graphite, Glassy Carbon, and Carbon Nanotubes Using Organic and Inorganic Voltammetric and X-ray Photoelectron Spectroscopy Labels

Charles A. Thorogood,[†] Gregory G. Wildgoose,[†] Alison Crossley,[‡] Robert M. J. Jacobs,[§] John H. Jones,[§] and Richard G. Compton*,[†]

Physical and Theoretical Chemistry Laboratory and Materials Department, Oxford University, South Parks Road, Oxford OX1 3QZ, United Kingdom, and Chemical Research Laboratory, Oxford University, Mansfield Road, Oxford OX1 3TA, United Kingdom

Received May 24, 2007. Revised Manuscript Received July 20, 2007

ortho-Quinones can be differentiated from other oxygen-containing surface functional groups on the surfaces of graphite, glassy carbon, "bamboo-like", and "hollow-tube" multiwalled carbon nanotubes and single-walled carbon nanotubes by chemically labeling them with either an inorganic hexamminechromium(III) complex or organic 1,2-phenylenediamine derivatives. Both types of labels can be observed using cyclic voltammetry or by X-ray photoelectron spectroscopy and used to quantify the numbers and relative distribution of *ortho*-quinones from other oxygen-containing species on the surface including electroactive *para*-quinones which are not labeled. Labeling of *ortho*-quinones with 1,2-phenylenediamine derivatives results in the formation of phenazine-like adducts on the graphitic surface which have a distinct voltammetry particularly from that of the underivatized *para*-quinones.

1. Introduction

Conducting forms of carbon such as graphite, glassy carbon (GC), carbon nanotubes (CNTs), and boron doped diamond (BDD) possess many desirable electrical, mechanical, physical, and chemical properties that have led to their widespread use in electrochemistry. As such they are often the electrode material of choice in many electrochemical applications such as in electroanalysis, catalysis, and fuel cells, to mention but a few.[1−4]

The surfaces of these materials, notably the graphitic forms of carbon (graphite, GC, and CNTs), are known to have a rich chemistry, with many different chemical functional groups naturally present on the surface, particularly at defect sites such as steps and edges.[2,3,5−8] In particular oxygen-containing surface functional groups, such as quinones/hydroquinones, hydroxyl, ketone, lactone, ether, and carboxyl groups, have been speculated to be present on graphitic surfaces.[2−4,6,9−11]

This surface functionality can also impart chemical reactivity to an otherwise inert graphitic surface, such that these surfaces can be chemically modified with a vast range of species using numerous synthetic strategies including, but not limited to, radical attack,[12−16] nucleophilic and electrophilic substitution,[17−23] acylation reactions (forming esters, thioesters, or amides),[24−30] electrostatic interactions,[31−35] physisorption,[14,36] and full or partial intercalation (see, for

* Corresponding author. E-mail: richard.compton@chem.ox.ac.uk. Tel: +44 (0)1865 275413. Fax: +44 (0)1865 275410.
[†] Physical and Theoretical Chemistry Laboratory.
[‡] Materials Department.
[§] Chemical Research Laboratory.

(1) Adams, R. N. *Electrochemistry at Solid Electrodes*; Marcel Dekker: New York, 1969.
(2) Banks, C. E.; Davies, T. J.; Wildgoose, G. G.; Compton, R. G. *Chem. Commun.* **2005**, 829.
(3) McCreery, R. L. Electroanalytical Chemistry. In *Electroanalytical Chemistry*, Bard, A. J., Ed.; Marcel Dekker: New York, 1991; Vol. 17, p 191.
(4) Wildgoose, G. G.; Banks, C. E.; Leventis, H. C.; Compton, R. G. *Microchim. Acta* **2006**, *152*, 187.
(5) Fan, Y.; Burghard, M.; Kern, K. *Adv. Mater.* **2002**, *14*, 130.
(6) Fryling, M. A.; Zhao, J.; McCreery, R. L. *Anal. Chem.* **1995**, *67*, 967.
(7) Chou, A.; Boecking, T.; Singh, N. K.; Gooding, J. J. *Chem. Commun.* **2005**, 842.
(8) Ji, X.; Banks, C. E.; Xi, W.; Wilkins, S. J.; Compton, R. G. *J. Phys. Chem. B* **2006**, *110*, 22306.
(9) Cline, K. K.; McDermott, M. T.; McCreery, R. L. *J. Phys. Chem.* **1994**, *98*, 5314.
(10) McDermott, C. A.; Kneten, K. R.; McCreery, R. L. *J. Electrochem. Soc.* **1993**, *140*, 2593.
(11) Ranganathan, S.; Kuo, T.-C.; McCreery, R. L. *Anal. Chem.* **1999**, *71*, 3574.
(12) Masheter, A. T.; Abiman, P.; Wildgoose, G. G.; E., W.; Xiao, L.; Rees, N. V.; Taylor, R.; Attard, G. A.; Baron, R.; Crossley, A.; Jones, J. H.; Compton, R. G. *J. Mater. Chem.* **2007**, *17*, 2616.
(13) Heald, C. G. R.; Wildgoose, G. G.; Jiang, L.; Jones, T. G. J.; Compton, R. G. *ChemPhysChem* **2004**, *5*, 1794.
(14) Leventis, H. C.; Streeter, I.; Wildgoose, G. G.; Lawrence, N. S.; Jiang, L.; Jones, T. G. J.; Compton, R. G. *Talanta* **2004**, *63*, 1039.
(15) Wildgoose, G. G.; Pandurangappa, M.; Lawrence, N. S.; Jiang, L.; Jones, T. G. J.; Compton, R. G. *Talanta* **2003**, *60*, 887.
(16) Strano, M. S.; Dyke, C. A.; Usrey, M. L.; Barone, P. W.; Allen, M. J.; Shan, H.; Kittrell, C.; Hauge, R. H.; Tour, J. M.; Smalley, R. E. *Science* **2003**, *301*, 1519.
(17) Thorogood, C. A.; Wildgoose, G. G.; Jones, J. H.; Compton, R. G. *New J. Chem.* **2007**, *31*, 958.
(18) Holm, A. H.; Moller, R.; Vase, K. H.; Dong, M.; Norrman, K.; Besenbacher, F.; Pedersen, S. U.; Daasbjerg, K. *New J. Chem.* **2005**, *29*, 659.
(19) Ghodbane, O.; Chamoulaud, G.; Belanger, D. *Electrochem. Commun.* **2004**, *6*, 254.
(20) Balaban, T. S.; Balaban, M. C.; Malik, S.; Hennrich, F.; Fischer, R.; Roesner, H.; Kappes, M. M. *Adv. Mater.* **2006**, *18*, 2763.
(21) Lee, H.-J.; Oh, S.-J.; Keum, D.-K.; Tan, L.-S.; Baek, J.-B. *Polym. Prepr.* **2005**, *46*, 199.

10.1021/cm071412a CCC: $37.00
Published on Web 09/12/2007

example, ref 4 for a review of many of these methods).[37,38] This makes these materials of interest to materials chemists and electrochemists alike, allowing one to "tailor-make" the properties of these materials in some desirable way for new materials applications, catalysis, sensors, and synthetic support materials. Furthermore the role of these oxygen-containing surface groups upon the electrode kinetics of graphite[9−11] and SWCNT[39] electrodes toward a wide variety of redox probes has been explored by several researchers.[9−11,40,41]

Most oxygen-containing functional groups are thought to be located at the edge-plane defect sites along the terminus of each graphene sheet at a step-edge defect on graphite, along the edges of the interwoven graphitic ribbons which form GC, and at the tube ends in CNTs. An ideal graphene sheet can terminate in two arrangements of the fused hexagonal rings which constitute it, the so-called "armchair" and "zigzag" configurations. In reality the edge is likely to have a rather more disordered structure with some disordered cross-linked cyclohexane- or pentane-like structures and amorphous regions in addition to oxygen-containing functionalities other than quinones. These oxygen-containing functional groups have been studied extensively using predominantly physical techniques including X-ray photoelectron spectroscopy (XPS),[42−47] thermal desorption methods,[48] vibrational spectroscopy,[6,49] NEXAFS,[50] and electrochemistry.[39,51−61]

Several researchers have studied the thermodynamics and kinetics of O_2 and H_2O chemisorption to form oxygen-containing functional groups on the zigzag edge of a graphite surfaces both theoretically and experimentally,[11,62−70] and this area is reviewed by Zhu et al.[71] Of note is the recent work of Sendt and Haynes who have used density functional theory to study the thermodynamics and kinetics of O_2 chemisorption on the armchair edge of graphite.[72] The formation of *ortho*-quinones on the same armchair ring is found to be energetically favorable, while chemisorption of O_2 across two adjacent rings leads predominantly to the formation of ketenes, furan-like structures, and ketone species which can also undergo energetically favorable migrations and rearrangements.[72]

Numerous studies have identified the presence of surface quinones in general, but to the best of our knowledge only one report so far has asked the question of how the quinone groups are distributed between *ortho*- and *para*-quinones. Schreurs et al. determined that the majority of quinone groups on the surface of the GC electrode pretreated with radio frequency plasma etching were *ortho*-quinones.[73] They achieved this by labeling *ortho*-quinone groups with 1,2-phenylenediamines to convert them into redox active benzophenazines in a similar manner to that reported herein.[73]

(22) Oh, S.-J.; Lee, H.-J.; Keum, D.-K.; Lee, S.-W.; Park, S.-Y.; Tan, L. S.; Baek, J. B. *Abstracts of Papers, 229th ACS National Meeting*, San Diego, CA, March 13−17, 2005; American Chemical Society: Washington, DC, 2005 (POLY).
(23) Tagmatarchis, N.; Georgakilas, V.; Tasis, D.; Prato, M.; Shinohara, H. *AIP Conf. Proc.* **2003**, *685*, 287.
(24) Liu, J.; Chou, A.; Rahmat, W.; Paddon-Row, M. N.; Gooding, J. J. *Electroanalysis* **2005**, *17*, 38.
(25) Gooding, J. J.; Wibowo, R.; Liu, J.; Yang, W.; Losic, D.; Orbons, S.; Mearns, F. J.; Shapter, J. G.; Hibbert, D. B. *J. Am. Chem. Soc.* **2003**, *125*, 9006.
(26) Wang, H.-j.; Peng, F.; Kuang, Z.-m.; Li, Z.-x.; Zhu, H.-c. *Tansu Jishu* **2004**, *23*, 10.
(27) Xiao, L.; Wildgoose, G. G.; Crossley, A.; Knight, R.; Jones, J. H.; Compton, R. G. *Chem. Asian J.* **2006**, *1*, 614.
(28) Sljukic, B.; Wildgoose, G. G.; Crossley, A.; Jones, J. H.; Li, J.; Jones, T. G. J.; Compton, R. G. *J. Mater. Chem.* **2006**, *16*, 970.
(29) Wildgoose, G. G.; Leventis, H. C.; Simm, A. O.; Jones, J. H.; Compton, R. G. *Chem. Commun.* **2005**, 3694.
(30) Wildgoose, G. G.; Leventis, H. C.; Davies, I. J.; Crossley, A.; Lawrence, N. S.; Jiang, L.; Jones, T. G. J.; Compton, R. G. *J. Mater. Chem.* **2005**, *15*, 2375.
(31) Zhao, L.; Liu, H.; Hu, N. *J. Colloid Interface Sci.* **2006**, *296*, 204.
(32) Zhang, M.; Gong, K.; Zhang, H.; Mao, L. *Biosens. Bioelectron.* **2005**, *20*, 1270.
(33) Guldi, D. M.; Prato, M. *Chem. Commun.* **2004**, 2517.
(34) Zhang, M.; Yan, Y.; Gong, K.; Mao, L.; Guo, Z.; Chen, Y. *Langmuir* **2004**, *20*, 8781.
(35) Guo, M.; Chen, J.; Nie, L.; Yao, S. *Electrochim. Acta* **2004**, *49*, 2637.
(36) Wildgoose, G. G.; Leventis, H. C.; Streeter, I.; Lawrence, N. S.; Wilkins, S. J.; Jiang, L.; Jones, T. G. J.; Compton, R. G. *ChemPhysChem* **2004**, *5*, 669.
(37) Wildgoose, G. G.; Hyde, M. E.; Lawrence, N. S.; Leventis, H. C.; Jiang, L.; Jones, T. G. J.; Compton, R. G. *Langmuir* **2005**, *21*, 4584.
(38) Wildgoose, G. G.; Wilkins, S. J.; Williams, G. R.; France, R. R.; Carnahan, D. L.; Li, J.; Jones, T. G. J.; Compton, R. G. *ChemPhysChem* **2005**, *6*, 352.
(39) Chou, A.; Boecking, T.; Singh, N. K.; Gooding, J. J. *Chem. Commun.* **2005**, 842.
(40) Banks, C. E.; Ji, X.; Crossley, A.; Compton, R. G. *Electroanalysis* **2006**, *18*, 2137.
(41) Ji, X.; Banks, C. E.; Crossley, A.; Compton, R. G. *ChemPhysChem* **2006**, *7*, 1337.
(42) Kozlowski, C.; Sherwood, P. M. A. *J. Chem. Soc., Faraday Trans. 1* **1984**, *80*, 2099.
(43) Kozlowski, C.; Sherwood, P. M. A. *J. Chem. Soc., Faraday Trans. 1* **1985**, *81*, 2745.
(44) Wandass, J. H.; Gardella, J. A.; Weinberg, N. L.; Bolster, M. E.; Salvati, L. *J. Electrochem. Soc.* **1987**, *134*, 2734.
(45) Blyth, R. I. R.; Buqa, H.; Netzer, F. P.; Ramsey, M. G.; Besenhard, J. O.; Golob, P.; Winter, M. J. *Appl. Surf. Sci.* **2000**, *167*, 99.
(46) Blyth, R. I. R.; Buqa, H.; Netzer, F. P.; Ramsey, M. G.; Besenhard, J. O.; Winter, M. J. *J. Power Sources* **2001**, *97−98*, 171.
(47) Estrade-Szwarckopf, H. *Carbon* **2004**, *42*, 1713.
(48) Fagan, D. T.; Kuwana, T. *Anal. Chem.* **1989**, *61*, 1017.
(49) Nakahara, M.; Sanada, Y. *J. Mater. Sci.* **1995**, *30*, 4363.
(50) Kuznetsova, A.; Popova, I.; Yates, J. T., Jr.; Bronikowski, M. J.; Huffman, C. B.; Liu, J.; Smalley, R. E.; Hwu, H. H.; Chen, J. G. *J. Am. Chem. Soc.* **2001**, *123*, 10699.
(51) Barbero, C.; Kötz, R. *J. Electrochem. Soc.* **1993**, *140*, 1.
(52) Barton, S. S.; Boulton, G. L.; Harrison, B. H. *Carbon* **1972**, *10*, 395.
(53) Blurton, K. F. *Electrochim. Acta* **1973**, *18*, 869.
(54) Blurton, K. F. *Electrochim. Acta* **1973**, *18*, 869.
(55) Elliott, C. M.; Murray, R. W. *Anal. Chem.* **1976**, *48*, 1247.
(56) Kepley, L. J.; Bard, A. J. *Anal. Chem.* **1988**, *60*, 1459.
(57) Liu, J.; Chou, A.; Rahmat, W.; Paddon-Row, M. N.; Gooding, J. J. *Electroanalysis* **2005**, *17*, 38.
(58) Szabo, T.; Berkesi, O.; Forgo, P.; Josepovits, K.; Sanakis, Y.; Petridis, D.; Dekany, I. *Chem. Mater.* **2006**, *18*, 2740.
(59) Zhang, D.; Sotomura, T.; Ohsaka, T. *Chem. Lett.* **2006**, *35*, 520.
(60) Zhu, J.-J.; Xu, J.-Z.; Hu, Z.; Chen, H.-Y. *Front. Biosci.* **2005**, *10*, 521.
(61) Pelekourtsa, A.; Missaelidis, N.; Jannakoudakis, D. *Chim. Chron.* **1997**, *26*, 39.
(62) Espinal, J. F.; Montoya, A.; Mondràgon, F.; Troung, T. N. *J. Phys. Chem. B* **2004**, *108*, 1003.
(63) Frankcombe, T. J.; Smith, S. C. *Carbon* **2004**, *42*, 2921.
(64) Montoya, A.; Mondràgon, F.; Troung, T. N. *Fuel Proc. Technol.* **2002**, *77−78*, 125.
(65) Montoya, A.; Mondràgon, F.; Troung, T. N. *J. Phys. Chem. A* **2002**, *106*, 4236.
(66) Montoya, A.; Mondràgon, F.; Troung, T. N. *Carbon* **2003**, *41*, 29.
(67) Radovic, L. R.; Bockrath, B. *J. Am. Chem. Soc.* **2005**, *127*, 5917.
(68) Sendt, K.; Haynes, B. S. *J. Phys. Chem. A* **2005**, *109*, 3438.
(69) Zhu, Z.; Finnerty, J.; Lu, G. Q. M.; Yang, R. T. *Energy Fuels* **2002**, *16*, 1359.
(70) Zhu, Z. H.; Finnerty, J.; Lu, G. Q.; Wilson, M. A.; Yang, R. T. *Energy Fuels* **2002**, *16*, 847.
(71) Zhu, Z. H.; Lu, G. Q.; Finnerty, J.; Yang, R. T. *Carbon* **2003**, *41*, 635.
(72) Sendt, K.; Haynes, B. S. *J. Phys. Chem. C* **2007**, *111*, 5465.
(73) Schreurs, J.; Van den Berg, J.; Wonders, A.; Barendrecht, E. *Recl.: J. R. Neth. Chem. Soc.* **1984**, *103*, 251.

Scheme 1. Structures of the Various Organic Phenylamine Derivatives Used To Label Quinone Groups Together with the Structures of the Two Model Quinone Compounds 9,10-Phenanthraquinone 6 and 9,10-Anthraquinone 7 and the Corresponding Adducts, 8 and 9, Respectively, Formed by Their Reaction with 1[a]

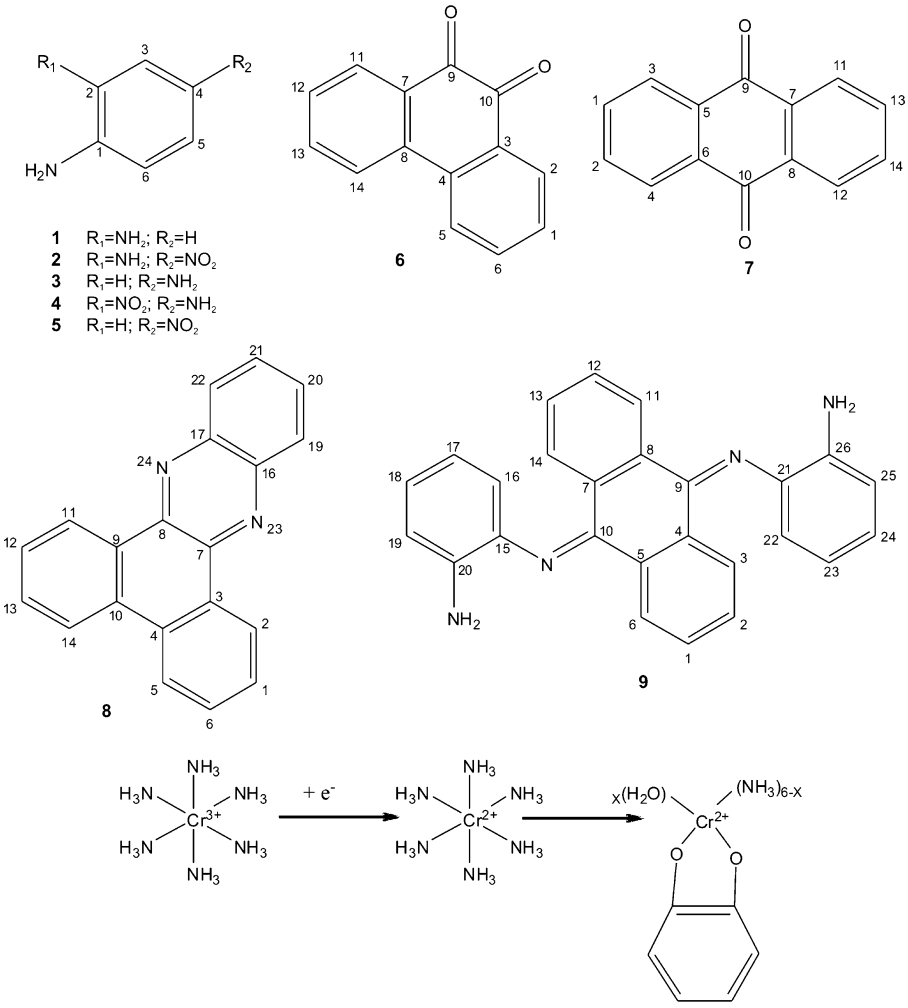

Another interesting method of electrochemically modifying carbon surfaces was developed and applied by Armstrong et al. via the reduction of an inorganic hexamminechromium-(III) complex.[74−77] Although the focus of their efforts was different to our own aims herein, they inadvertently developed a method by which *ortho*-hydroquinone groups could be labeled with chromium(II/III), which we have also exploited herein.

Recently we have developed several *chemical* as opposed to physical methods to label and identify radical sites,[12] carboxyl groups,[78] and also aliphatic (ketones) and aromatic (quinones) carbonyl containing species on the surfaces of graphite and CNTs of various morphologies.[17] Each functional group was chemically labeled with a species that could be explored using voltammetry, XPS, or both.

In this report we will adapt the method of Armstrong et al. to label *ortho*-quinone structures on the surfaces of graphite, GC, BDD, and three morphologies of CNTs, namely, "bamboo-like" and "hollow-tube" multiwalled CNTs (b-MWCNTs and h-MWCNTs, respectively) and single-walled CNTs (SWCNTs). The presence of any complex formed between the hexamminechromium(III) and *ortho*-quinones on these surfaces (Scheme 1) can be identified both voltammetrically and using XPS. Furthermore, we also label *ortho*-quinones on the surface of graphite, GC, and h-MWCNT powders with a variety of 1,2-phenylenediamine derivatives, **1** and **2**, using classical organic synthetic techniques (Scheme 1), to form voltammetrically active phenazine derivatives, which can also be detected using XPS. The adduct of the various phenylenediamine derivatives **1** and **2** with *ortho*-quinones is differentiated from any adducts formed with *para*-quinone species via a series of detailed control experiments using derivatives **3** and **5**.

2. Experimental Section

2.1. Reagents and Equipment. All reagents were obtained from Aldrich (Gillingham, U.K.) with the exception of potassium chloride (Reidel de Haën, Seelze, Germany), were of the highest commercially available grade, and were used without further purification. Bamboo-like and hollow-tube multiwalled CNTs (b-MWCNT and h-MWCNTs, respectively, 30 ± 15 nm diameter, 5−20 μm length, <95% purity) were purchased from Nanolab (Brighton,

(74) Armstrong, F. A.; Cox, P. A.; Hill, H. A. O.; Oliver, B. N.; Williams, A. A. *J. Chem. Soc., Chem. Commun.* **1985**, 1236.
(75) Armstrong, F. A.; Hill, H. A. O.; Oliver, B. N. *J. Chem. Soc., Chem. Commun.* **1984**, 976.
(76) Armstrong, F. A.; Hill, H. A. O.; Oliver, B. N.; Walton, N. J. *J. Am. Chem. Soc.* **1984**, *106*, 921.
(77) Armstrong, F. A.; Hill, H. A. O.; Oliver, B. N.; Whitford, D. *J. Am. Chem. Soc.* **1985**, *107*, 1473.
(78) Masheter, A. T.; Xiao, L.; Wildgoose, G. G.; Crossley, A.; Jones, J. H.; Compton, R. G. *J. Mater. Chem.* **2007**, *33*, 3515.

MA). SWCNTs produced using the HiPCO method (1−2 nm diameter, 2−5 μm in length) were purchased from Carbon Nanotechnologies Inc. (U.S.A.). Highly ordered pyrolytic graphite (HOPG) was purchased from SPI 1, equivalent to the highest quality ZYA grade made by Union Carbide.[79]

Electrochemical measurements were carried out using an μAutolab computer controlled potentiostat (Ecochemie, Utrecht, The Netherlands) in a cell of volume 25 cm^3 using a three-electrode configuration. The working electrode consisted of either (i) a basal-plane or (ii) an edge-plane pyrolytic graphite electrode (bppg and eppg, respectively, area = 0.025 cm^2, Le Carbone, Brighton, Sussex, U.K.), (iii) a GC electrode (GC, 3 mm diameter, BAS Technicol, U.K.), or (iv) a BDD electrode (BDD, 5 mm × 5 mm, Windsor Scientific, Slough, Berkshire, U.K.). For electrochemical experiments coupled with XPS (see below), a specially designed bppg, eppg, or GC "stub" electrode was used. These consisted of 3 mm discs of each material mounted in a poly(tetrafluoroethylene) (PTFE) stub, 10 mm in diameter and 7 mm high with a stainless steel plate on the reverse side of the electrode. These stubs could be interchangeably mounted in a PTFE screw-threaded holder, with electrical contact made by a brass pin. After electrodeposition, each electrode stub could be removed from the housing and mounted in the spectrometer. In all cases a bright platinum wire coil acted as the counter electrode and a saturated calomel reference electrode (SCE, Radiometer, Copenhagen, Denmark) completed the cell assembly. Cyclic voltammetry (CV) was recorded at a scan rate of 100 mV s^{-1} and step potential of 2 mV unless stated otherwise. All solutions were prepared using deionized water (Vivendi, Millipore, resistivity not less than 18.2 MΩ cm at 25 °C) and were thoroughly degassed with pure N_2 or saturated with NH_3 (BOC gases, Guildford, Surrey, U.K.) for 15 min prior to performing any voltammetric measurements (see below).

XPS was performed using a VG Clam 4 MCD analyzer system at the OCMS Begbroke Science Park, University of Oxford, U.K., using X-ray radiation from the Al Kα band ($h\nu$ = 1486.7 eV). All XPS experiments were recorded using an analyzer energy of 100 eV for survey scans and 20 eV for detailed scans with a takeoff angle of 90°. The base pressure in the analysis chamber was maintained at not more than 2.0×10^{-9} mbar. Each sample was mounted on a stub using double-sided adhesive tape and then placed in the ultrahigh vacuum analysis chamber of the spectrometer. To prevent the sample from becoming positively charged when irradiated due to emission of photoelectrons, the sample surface was bombarded with an electron beam (10 eV) from a "flood gun" within the analysis chamber of the spectrometer. Analysis of the resulting spectra was performed using Microcal Origin 6.0. Assignment of the spectral peaks was made using the UKSAF[80] and NIST[81] databases.

In situ atomic force microscopy (in situ AFM) was performed using a Digital Instruments (Santa Barbara, CA) Multimode scanning probe microscope, operating in contact mode with an "E" scanner, having a lateral range of 12 × 12 μm and a vertical range of 3 μm. Standard silicon nitride probe tips were used (Veeco Nanoprobe Tip, model NP-S20, Veeco, Woodbury, NY), having a force constant of approximately 0.58 N m^{-1}. In situ AFM experiments were performed in a Digital Instruments fluid cell (having an approximate volume of 0.5 cm^3. Once in position on the AFM scanner head, the solution was fed into one of the inlets of the cell using a syringe until it was full and no bubbles remained. Each AFM image was analyzed as a 256 × 256 array of heights in nanometers, with heights measured relative to the mean plane of the image.

(79) http://www.2spi.com/catalog/new/hopgsub.shtml, 2003.

One-dimensional ^{1}H NMR experiments were performed on a Bruker AVB500 500 MHz instrument using deuterated dimethyl sulfoxide (DMSO-d_6) as the solvent. All chemical shifts are reported relative to tetramethyl silane (TMS) as a standard.

2.2. Synthesis of Hexamminechromium(III) Nitrate. Hexamminechromium(III) nitrate was synthesized by adapting the method of Oppegard and Bailar as follows:[82] 62.5 mg of sodium metal was dissolved in 100 cm^3 of liquid ammonia (−33 °C) forming a rich blue solution to which 25 mg of iron(II) ammonium sulfate was then added until the blue solution had become colorless. Next 1 g of chromium(III) chloride was added to the solution in 0.25 g portions at approximately 3 min intervals with stirring. After the addition was complete the liquid ammonia was allowed to evaporate and the resulting brown solid residue was transferred to a large crystallizing dish. It was allowed to stand with occasional stirring until the odor of ammonia was gone leaving 1.55 g of a bright yellow free flowing powder of impure hexamminechromium(III) chloride.

The impure solid $[Cr(NH_3)_6]Cl_3$ was then dissolved in 15 cm^3 of pure water (at 40 °C) containing 1 cm^3 of concentrated HCl. Concentrated nitric acid (5 cm^3) was then added, and the solution was allowed to cool to room temperature, precipitating pure hexamminechromium(III) nitrate. After standing for a few minutes, the bright yellow crystalline salt was collected on a Buchner funnel and washed with cold distilled water containing a little nitric acid, then with ethanol, and finally with ether. The product was dried overnight in a vacuum desiccator and stored in a dark bottle at 4 °C prior to use. Approximately 1.5 g of the purified $[Cr(NH_3)_6](NO_3)_3$ product was collected (ca. 70% yield). The material was characterized using XPS as described in the Supporting Information.

2.3. Coupling of Phenylenediamine Compounds to Quinones. The coupling of individual reactants **1**−**5** to quinone groups on the surface of each carbonaceous material studied was achieved using an adaptation of a classical synthesis:[83,84] A 1 mM solution of the selected compound was prepared in 1 cm^3 of ethanol. This was added to a suspension of the carbonaceous material (0.1 g in the case of graphite and GC powder and 0.025 g in the case of h-MWCNT) in 7 cm^3 of warm glacial acetic acid and heated with stirring for 30 min at 100 °C. The resulting modified carbonaceous material was then filtered under suction and washed rigorously with hot ethanol, acetone, acetonitrile, and finally deionized water to remove any unreacted, physisorbed species and any acetic acid. In the case of the formation of adducts **8** or **9** the product was washed with ethanol and deionized water only to avoid dissolution of the product. The product was then dried in an oven at 100 °C. Where the coupling of **1**−**5** was carried out directly on a carbonaceous electrode substrate (bppg, eppg, GC, or BDD) the electrode itself was suspended in the reaction mixture in place of the carbonaceous powder. For the reaction of **1** with 9,10-phenanthraquinone **6** or 9,10-anthraquinone **7** the reaction was carried out as described above except that a 1 mM solution of **6** or **7** in the warm glacial acetic acid replaced the carbonaceous powder material, to form the adducts **8** and **9**, respectively.

3. Results and Discussion

3.1. Voltammetric Labeling of *ortho*-Quinones Using Hexamminechromium(III) Nitrate. Two methods of modi-

(80) http://www.uksaf.org/, 2003.
(81) http:srdata.nist.gov/xps/, 2003.
(82) Oppegard, A. L.; Bailar, J. C. *Inorg. Synth.* **1950**, *3*, 153.
(83) Hinsberg, O. *Annalen* **1887**, *237*, 327.
(84) Fitton, A. O.; Smalley, R. K. *Practical Heterocyclic Chemistry*; Academic Press Inc.: London, 1968.

fying the surface of an eppg electrode were investigated on the basis of the method of Armstrong et al.[74] using a 10 mM aqueous solution of hexamminechromium(III) nitrate. First the potential was cycled from +1.0 V to −1.4 V versus SCE at 20 mV s^{-1} in the chromium solution which was first saturated with ammonia to reduce the degree of substitution of the labile chromium(II) intermediate by water molecules. A large cathodic peak could be observed at approximately −1.3 V, which is similar to the reported polarographic reduction potential of the hexamminechromium(III) complex. A proportion of the resulting labile hexamminechromium-(II) species can then coordinate to any surface *ortho*-hydroquinones as proposed in Scheme 1, before being rapidly reoxidized back to form a surface-bound, substitution-inert chromium(III) complex on the eppg surface. Two additional oxidative voltammetric peaks could also be observed in the first scan at −0.655 and −0.640 V (Supporting Information, Figure 2) which, on subsequent scans, exhibited quasi-reversible reduction peaks at similar potentials. By comparison to the work of Ji et al. these can be attributed to the reduction and subsequent reoxidation of ammonium ions and protons, respectively.[40,85−87] A further smaller and broader wave appeared on the oxidative scan at approximately +0.5 V which was not present if the electrode was cycled over a similar potential range in the absence of the hexamminechromium(III) complex (see below). The presence of the voltammetric waves due to the redox behavior of the ammonium ion is an unwanted complication, especially as Ji et al. have demonstrated that under very reducing potentials a degree of intercalation of NH_4^+ ions can occur, leading to exfoliation and disruption of the eppg electrode surface.[85−88] Therefore the above experiment was repeated without presaturating the solution with ammonia. Figure 3 in the Supporting Information shows the resulting cyclic voltammogram. Again the large reduction peak corresponding to the reduction of the chromium(III) complex can be observed, and again a small voltammetric wave can be observed when the potential is scanned in the oxidative direction at approximately +0.5 V.

The second method of modifying a carbon electrode with chromium(III) is to simply poise the electrode potential at −1.35 V versus SCE for 60 s, and again this method was adapted to avoid presaturating the solution with ammonia. After this time, the electrode is removed from the chromium containing solution, rinsed with deionized water, and placed into a solution of 0.1 M KCl. Figure 4 in the Supporting Information shows the resulting voltammetry compared to that of an eppg electrode which had been treated under identical conditions but in the absence of any chromium species. Using this modification method a new oxidative voltammetric peak is again observed at +0.75 V versus SCE, which upon cycling in a reductive direction exhibits a corresponding reduction wave at approximately 0.25 V, in approximately a 1:1 ratio of peak areas and with a wave shape characteristic of a surface bound species, indicating that the chromium species is surface bound and undergoes a quasi-reversible redox process. Upon repetitive cycling the oxidative and reductive waves were found to decrease in height and broaden, while maintaining the same peak area (i.e., no material is desorbing from the electrode surface). The reduction was also found to gradually shift to less positive potentials while broadening, possibly as a result of the formation of two partially deconvoluted waves corresponding to a gradual conversion of one form of the complex species to another as discussed below. What is apparent from the control experiment using an eppg electrode which had been pretreated in the absence of any chromium species is that this new redox system must correspond to the modification of the carbon surface with a chromium complex.

Determining the exact nature of this surface-bound chromium species is beyond the scope of this report. However, assuming that it is a chromium species bound to an *ortho*-quinone group (see below), there are two mechanisms that could tentatively be proposed to explain the observed redox behavior. Pierpont et al. have studied the redox behavior of tris and bis *o*-quinone and semiquinone-catecholate complexes of chromium(III) in nonaqueous electrolytes, using derivatives of the model ligand 9,10-phenanthraquinone.[89,90] These complexes exhibit several redox waves attributed to the sequential one-electron conversions of quinone to semiquinone to catecholate species which involve changes in the π^* occupancy of the ligand rather than changes in the oxidation state of the metal center. In aqueous solutions quinones usually undergo such transformations in a single two-electron step. Thus it can be postulated that the redox waves observed herein can be attributed to the two-electron quasi-reversible redox behavior of the coordinated *ortho*-quinone in the $[Cr(NH_3)_{4-x}(OH_2)_x(\textit{ortho}\text{-quinone})]^{3+}$ complex shown in Scheme 1. However, this mechanism does not explain why the peaks should broaden and their peak potentials shift. Alternatively, the observed redox waves lie at potentials at which the oxidation of certain related chromium complexes is known, forming Cr(V) complexes.[91] Intermediate chromium(IV) complexes are also known, but unless the Cr(IV) center is stabilized by more than one ligand of the (*phen*) type, then these intermediates are unstable with respect to disproportionation to Cr(III)/Cr(V).[89−91] The formation of Cr(V) complexes may lead to oxidation of the complexed ligands, with aqua ligands forming oxo (Cr═O) species and any remaining amino ligands either undergoing substitution with water or forming amido species (Cr═NH), which may explain the broadening and slight shift in the redox potentials of the reduction wave on successive scans. In either mechanism the redox process is tentatively postulated to involve the net transfer of two electrons.

The method of poising the electrode potential described above produced larger, more clearly resolved waves than the potential cycling method and was therefore used throughout.

(85) Compton, R. G.; Banks, C. E.; Ji, X. Detection of ammonia by electrodes comprising glassy carbon or boron-doped diamond. PCT Int. Appl. (2007), 29 pp. CODEN: PIXXD2 WO 2007020410 A1 20070222.
(86) Ji, X.; Banks, C. E.; Hu, G.; Crossley, A.; Compton, R. G. *Electroanalysis* **2006**, *18*, 2141.
(87) Ji, X.; Banks, C. E.; Compton, R. G. *Electroanalysis* **2006**, *18*, 449.
(88) Ji, X.; Banks, C. E.; Silvester, D. S.; Wain, A. J.; Compton, R. G. *J. Phys. Chem. C* **2007**, *111*, 1496.
(89) Downs, H. H.; Buchanan, R. M.; Pierpont, C. G. *Inorg. Chem.* **1979**, *18*, 1736.
(90) Buchanan, R. M.; Claflin, J.; Pierpont, C. G. *Inorg. Chem.* **1983**, *22*, 2552.
(91) Gould, E. S. *Coord. Chem. Rev.* **1994**, *135−136*, 651.

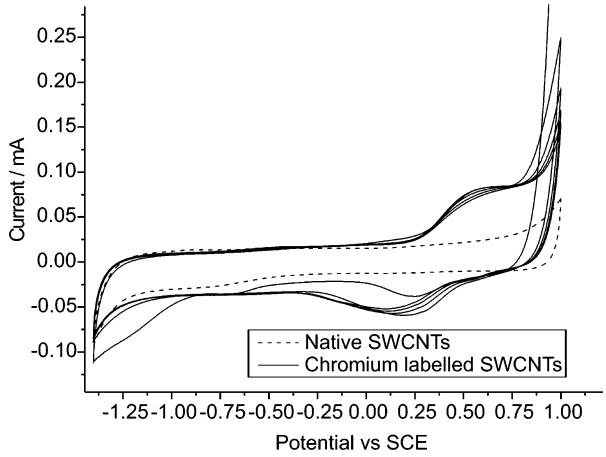

Figure 1. Overlaid cyclic voltammograms recorded in 0.1 M KCl of native SWCNTs and SWCNTs after labeling with hexamminechromium(III) (first five cycles). The SWCNTs were abrasively immobilized onto a bppg electrode. Scan rate 100 mV s^{-1}.

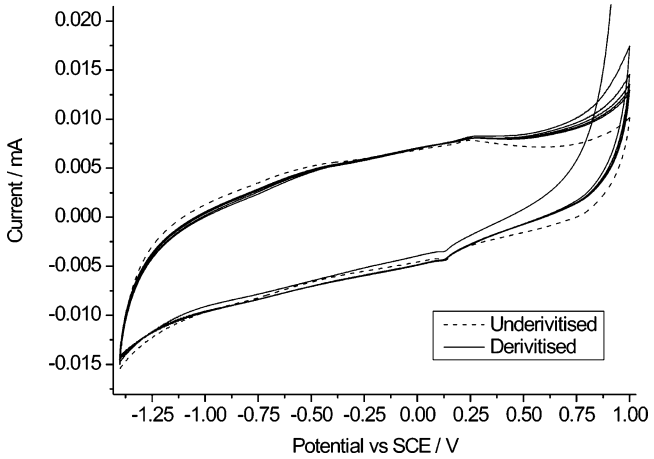

Figure 2. Overlaid cyclic voltammograms recorded in 0.1 M KCl of a GC electrode before and after labeling with hexamminechromium(III) (first five cycles), recorded at a scan rate of 100 mV s^{-1}.

Next, a bppg, BDD, and GC electrode surface was modified as described above as well as b-MWCNTs, h-MWCNTs, and SWCNTs which were abrasively immobilized onto the surface of a bppg electrode. With the exception of the GC and BDD electrodes, discussed below, the other graphitic electrodes studied all showed the same qualitative behavior as that seen at the eppg electrode, the only difference being the magnitude of the observed peak currents corresponding to the chromium complex, reflecting the different amounts of *ortho*-quinone groups present and/or the different electrode areas or amounts of immobilized CNT materials on the electrode surface. Figure 1 shows the resulting response for the case of the SWCNTs. In the case of the BDD electrode no voltammetry corresponding to the surface bound chromium species or any other surface functionality could be observed in the potential window of interest.

Figure 2 shows the response of the chromium(III) modified and unmodified GC electrode in 0.1 M KCl solution. For the GC electrode modified in the presence of hexamminechromium(III) nitrate no voltammetry corresponding to the surface bound chromium complex can be observed. However, in the voltammetry of both the "modified" and bare electrode a small, quasi-reversible redox couple can be observed at

Table 1. Surface Coverage of Quinone Groups on Each Carbonaceous Material Studied As Determined Using Voltammetric Labeling with the Hexamminechromium(III) Complex

material	surface coverage of *ortho*-quinones (mol cm^{-2})
eppg	1.7×10^{-10}
bppg	2.0×10^{-12}
GC	
b-MWCNTs	3.2×10^{-12}
h-MWCNTs	2.5×10^{-12}
SWCNTs	5.1×10^{-13}

approximately +0.13 V versus SCE, which, from previous studies,[92−97] is likely to be attributed to electroactive surface species such as quinone groups which have not been labeled with chromium, likely comprising *para*-quinones. This conclusion is supported by considering that the *ortho*-quinone groups are acting as a bi-dentate ligand whereas the *para*-quinones are in effect mono-dentate. Therefore, this "chelate effect" ensures that the binding of the *ortho*-quinone groups to the chromium(III) center is entropically favored over the binding of *para*-quinone groups.

The surface coverage, Γ, of labeled *ortho*-quinone groups on each carbonaceous electrode surface studied was calculated (Table 1) by measuring the reductive peak area (the oxidative peak is obscured by the onset of solvent breakdown making it difficult to accurately measure) using eq 1:

$$\frac{Q}{nFA} = \Gamma \tag{1}$$

where Q is the peak area/C, n is the number of electrons transferred assumed to be equal to 2, F is the Faraday constant 96 485 C mol^{-1}, and A is the geometric electrode area. In the case of CNTs immobilized onto a bppg electrode the area was estimated as described in our previous work.[12,17] The surface coverage and distribution of each type of oxygen-containing functionality on carbon surfaces varies strongly with the morphology of the material and its method of manufacture, storage, and pretreatment.[3,9−11] Therefore it is less instructive to report absolute values, but the results of Table 1 allow us to make a comparison with estimates of the surface coverage of *ortho*-quinones obtained using other methods (XPS and labeling with organic molecules, see below) as well as other surface functional groups determined using a variety of voltammetric and XPS labels used in our previous work.[17,78]

The lack of any chromium-labeled groups on the GC surface is both interesting and alarming as GC surfaces are known to be decorated with significant numbers of quinone groups among other oxygen-containing groups such as carboxyl.[3] One further possibility is that the proposed mechanism of Armstrong et al. whereby the hexamminechromium(III) complex labels *ortho*-quinone groups is incorrect. It is possible that the observations described above could be explained by an alternative mechanism involving the full or partial intercalation of the chromium species

(92) Masheter, A. T.; Wildgoose, G. G.; Crossley, A.; Jones, J. H.; Compton, R. G. *J. Mater. Chem.* **2007**, *17*, 3008.
(93) Maruyama, J.; Abe, I. *Electrochim. Acta* **2001**, *46*, 3381.
(94) Dai, H.-P.; Shiu, K.-K. *J. Electroanal. Chem.* **1996**, *419*, 7.
(95) Yang, Y.; Lin, Z. *Synth. Met.* **1996**, *78*, 111.
(96) Zagudaeva, N. M. *Elektrokhim.* **1986**, *22*, 1697.
(97) Vasquez, R. E.; Imai, H. *Bioelectrochem. Bioenerg.* **1985**, *14*, 389.

Table 2. Elemental Surface Composition of an eppg, bppg, and GC Electrode Labeled with the Hexamminechromium(III) Relative to the C(1s) Peak (as 100%) and after Correction To Take into Account the Emission from the PTFE Surrounding Mantle[a]

electrode material	% Cr ± 0.05%	% O ± 0.05%	% N ± 0.05%	% of the total O(1s) peak attributed to *ortho*-quinones
eppg	3.54	36.33	2.33	19.5
bppg	1.62	48.51	3.34	13.8
GC	0.61	21.11	1.92	5.8

[a] Correlated to the F(1s) peak. Also shown is the percentage of the total O(1s) peak attributed to *ortho*-quinone groups.

between the constituent graphene sheets in the graphite and MWCNT materials or between the interstices in bundles of SWCNTs, driven by the application of such a large negative electrode potential. To test this hypothesis in situ AFM was performed on a HOPG electrode as any effects of full or partial intercalation can easily be observed in "real time" as a change in step-defect heights and/or deformation of the relatively pristine electrode surface.[37] The results of these experiments are presented in the Supporting Information and lead us to conclude that the proposed mechanism of Armstrong et al. is likely to be correct and that the only way in which the chromium complex can modify the carbon surface is by coordination to adjacent surface oxygen groups such as those found in *ortho*-quinone groups.

3.2. XPS Labeling of *ortho*-Quinones Using Hexamminechromium(III) Nitrate. The previous sections have developed the use of hexamminechromium(III) nitrate as a voltammetric label for *ortho*-quinones on graphitic surfaces. In this section we explore the use of hexamminechromium(III) as an XPS label. To this end, bppg, eppg, and GC electrode stubs were modified by poising the electrode potential in a 10 mM hexamminechromium(III) nitrate solution as described above. The electrodes were then thoroughly rinsed with deionized water to remove any adsorbed chromium species and allowed to dry before being mounted in the XPS spectrometer. Survey scans were performed from 0 to 1200 eV as shown in Figures 5 and 6 in the Supporting Information. In each case several spectral peaks could be observed which were assigned to the C(1s), N(1s), O(1s), Cr(2p) (split by spin orbit coupling into $j = 1/2$ and $j = 3/2$ levels), F(1s), and Auger emissions from the KLL levels of O, F, and C atoms at higher binding energies, using the NIST[81] and UKSAF[80] databases. The presence of trace Si impurities, which are also observed as emission from the Si(2p) levels, is likely to be due to embedded SiC microparticles incorporated into the electrode surface during its preparation. The significant F(1s) peak is due to the X-ray beam spot size being slightly greater than that of the electrode stub and corresponds to emission from the surrounding PTFE mantle. From the C(1s), O(1s), N(1s), and Cr(2p) spectral peaks the percentage elemental composition of each surface relative to the C(1s) signal can be calculated, after taking into account both the relative cross-sectional area of each element[80] and the contribution to the C(1s) signal from the surrounding PTFE mantle (correlated to the F(1s) signal), and are reported in Table 2.

It is apparent that a significantly greater amount of chromium is incorporated onto the eppg and bppg electrodes compared to the GC electrode in agreement with the voltammetric studies above. Furthermore, from the percentage elemental nitrogen present on the surface it is clear that substantial substitution of the amine ligands by water molecules has occurred during the reduction of the Cr(III) complex to the labile Cr(II). Consideration of the contribution of these aqua ligands to the O(1s) signal has been neglected as their coordination number to the chromium complex is variable; the small error introduced by neglecting these groups is negligible (<3%) especially as, for reasons discussed above, we are not interested in assigning *absolute* values of surface coverage of each functional group present on the surface; rather, we are interested in showing that this methodology is a useful tool for "mapping" the surface functionality on carbon surfaces and for *relative* comparisons of different materials.

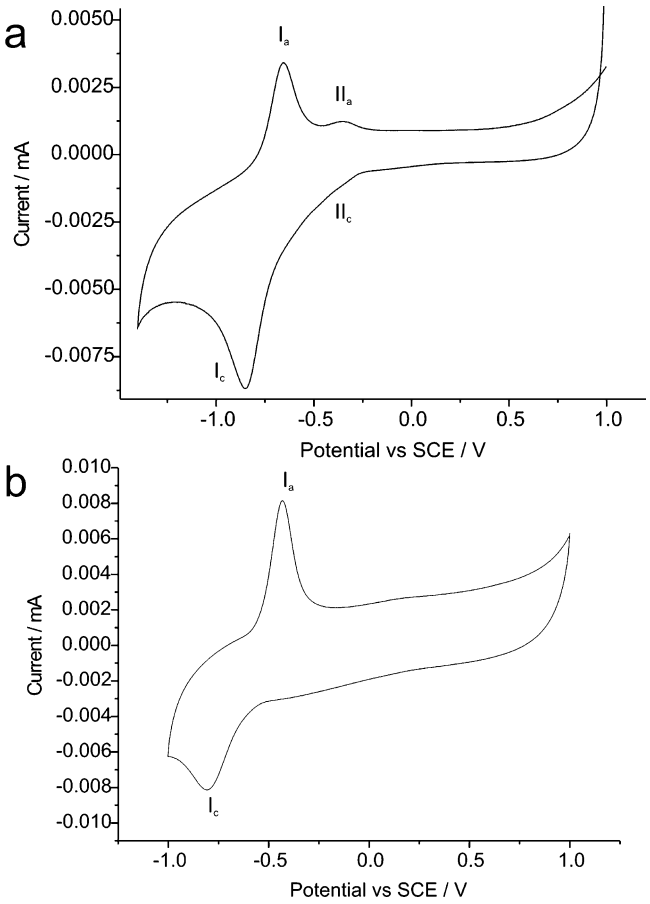

Figure 3. Cyclic voltammetric response (first scan) of the model adduct **8**, in (a) 0.1 M KCl and (b) in pH 6.8 phosphate buffer solution recorded at 100 mV s^{-1}.

Assuming that each chromium ion is coordinated to two quinone carbonyl groups, we can estimate the amount of *ortho*-quinone groups on each surface as a percentage of the *total* oxygen-containing functionalities on each surface, and this is also included in Table 2.

3.3. Voltammetric Labeling of *ortho*-Quinones with 1,2-Phenylenediamines. Having described one method of labeling *ortho*-quinones on carbon surfaces using an inorganic voltammetric and XPS label, we now turn to a complimentary method using an organic label which exploits the well-known reaction of 1,2-phenylenediamines with *ortho*-quinones to form phenazine derivatives.[84]

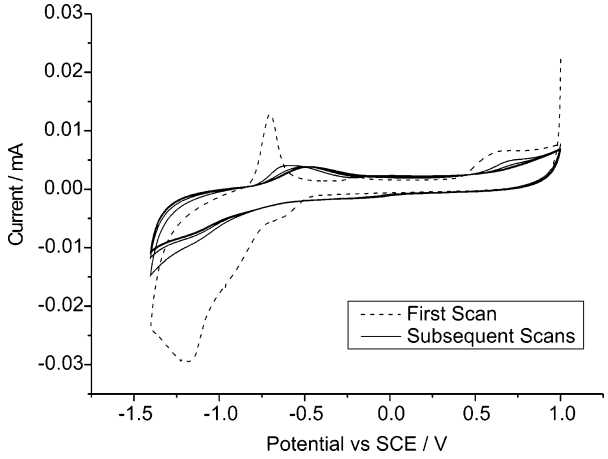

Figure 4. Cyclic voltammetric response of the nitro derivative of model adduct **8**, in 0.1 M KCl recorded at 100 mV s^{-1}.

3.3.1. Comparison with Model Compounds. To first voltammetrically characterize the phenazine adducts formed by reaction of **1** with *ortho*-quinones, as outlined in section 2.3, the model compound **6** was reacted with **1** to form the crystalline product **8**. The adduct formation was confirmed by comparing the ^{1}H NMR spectrum of **8** with the literature[98] as described in the Supporting Information. The resulting adduct **8** was abrasively immobilized onto a bppg electrode, and CV was recorded in 0.1 M KCl and in pH 6.8 phosphate buffer (Figure 3a,b). A quasi-reversible redox couple (labeled I_a and I_c in Figure 3a) with a wave shape characteristic of a surface bound species can be observed centered at approximately −0.8 V versus SCE in excellent agreement with the literature reports for benzo[*a*,*c*]phenazine[99−103] itself and other phenazine derivatives such as neutral red,[104−107] corresponding to the two-electron, two-proton reduction of the phenazine ring as shown in Scheme 2. Depending on the solution pH the reduction can occur as a single two-electron, two-proton transfer or two sequential single electron transfers with concomitant protonation which results in two closely spaced voltammetric waves being observed. This can be used to explain why in unbuffered 0.1 M KCl a second smaller oxidative and cathodic wave labeled as IIa and IIc in Figure 4a can be observed centered at slightly more positive potentials.

In addition to labeling surface quinones with **1**, we also chose to label them with the nitro derivative of **1**, namely, compound **2** in Scheme 1, as these compounds have a distinct voltammetric response and also will give rise to a more intense N(1s) emission in XPS. The presence of the electron withdrawing nitro group in the 4-position is known to decrease the nucleophilicity of the amine group in the 2-position (but not the amine group in the 1-position) and therefore slows down the rate of phenazine formation by approximately a factor of 10^3 compared to that of **1**. Therefore we also reacted **2** with **6** to form the corresponding nitro derivative of adduct **8**. The ^{1}H NMR spectrum of the nitro derivative of **8** (Supporting Information) revealed that the phenazine ring formation still occurs on the time scale of the reaction.[108] The corresponding voltammetry is shown in Figure 4. In aqueous media aryl nitro compounds can either undergo an electrochemically and chemically irreversible four-electron, four-proton reduction to form a new redox couple corresponding to the two-electron, two-proton quasi-reversible arylnitroso/arylhydroxylamine redox couple, or depending on the substituent groups on the aryl ring, complete reduction to form the corresponding arylamine can occur in a six-electron, six-proton step.[109−112]

Upon first scanning in the reductive direction a large irreversible reduction wave can be observed at −1.16 V versus SCE, which is co-incident with the reduction peak corresponding to any phenazine rings (this peak can be seen as a slight shoulder on the nitro reduction wave at ca. −0.9 V). Upon reversing the scan direction the appearance of the single oxidative wave of the phenazine couple can be observed. No new redox couples were observed at potentials which correspond to the formation of an arylnitroso/arylhydroxylamine couple, indicating that in this case complete reduction of the nitro group to the corresponding amine occurs in a six-electron, six-proton reduction step. This is confirmed by the presence of an irreversible oxidation peak at approximately 0.6 V corresponding to the oxidation of the aromatic amine functionality.[109−112] Upon subsequent scans the reduction wave corresponding to the arylnitro group is no longer present, and the reduction wave corresponding to the phenazine couple can now be observed at similar potentials to that seen for **8** in Figure 3. For both compound **1** and compound **2** this confirms the formation of phenazine species with *ortho*-quinones under the reaction conditions employed herein. One final control was performed by

Scheme 2. Reduction Mechanism of Benzo[*a*,*c*]phenazine Showing both the Simultaneous Two-Electron, Two-Proton Single Redox Wave Process and the Low pH Mechanism Where Intermediate Protonation Steps Produce Two Separate Voltammetric Waves[a]

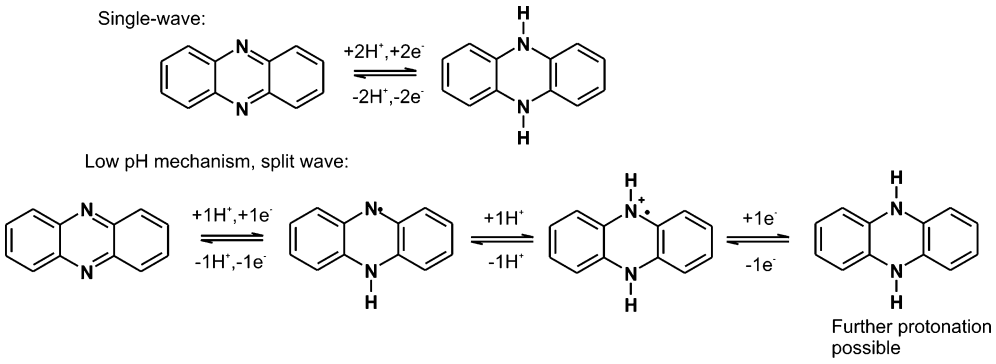

[a] The order of electron and proton transfers may differ from that shown and further protonation of the reduced product may occur.

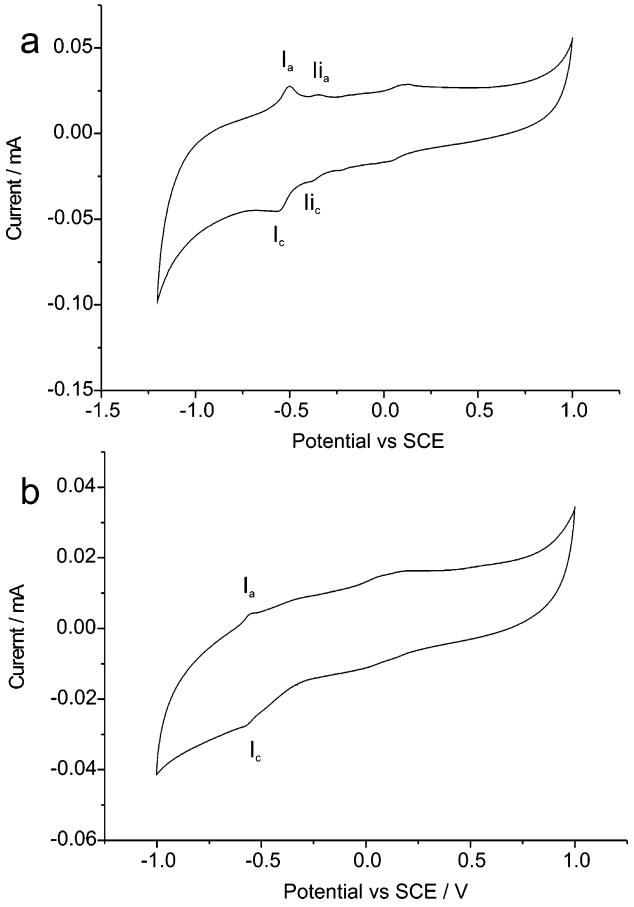

Figure 5. Cyclic voltammetric response of (a) graphite powder and (b) GC powder labeled with **1** in 0.1 M KCl.

coupling **1** with **7** to form the adduct **9**. The voltammetric response (not shown) of this adduct was markedly different from that of any phenazine derivative species, with no voltammetric peaks observed which would obscure the region of interest around the potentials where phenazine redox processes occur.

3.3.2. Voltammetric Labeling of Surface ortho-Quinones on Graphite and GC Surfaces. Having confirmed that compounds **1** and **2** can be used to label *ortho*-quinones by forming the phenazine rings with a distinctive voltammetry, we next derivatized graphite and GC powders with both **1** and **2** as described in section 2.3. The modified carbon powders were then abrasively immobilized onto a bppg electrode and studied using CV as shown in Figure 5a,b. In the case of the labeled graphite powder (Figure 5a) a quasi-reversible set of voltammetric peaks, labeled I_a/I_c, with a smaller set of peaks (II_a/II_c) just discernible at slightly more positive potential are observed at potentials almost identical to that observed in the voltammetry of **8** above. By comparison with **8** above, system I is characteristic of the formation of a surface bound phenazine species, arising from the chemical labeling of *ortho*-quinone groups on the surface of graphite with **1**. The peaks labeled as system II are observed in the voltammetry of blank graphite and are probably due to impurities in the graphite, such as sulfides, which are introduced from the petroleum based hydrocarbon feedstock used during manufacture of the synthetic graphite powder. A further, poorly resolved redox process can be observed at approximately 0 V versus SCE (labeled as III_a/III_c). This is commonly observed in the voltammetry at graphite electrode (frequently but erroneously described in the literature as a "pseudo-capacitance") and is attributed to the quasi-reversible two-electron, two-proton behavior of the surface quinone/hydroquinone redox couple.[92,94−97] Assuming that the derivatization reaction is quantitative and all the *ortho*-quinone groups on the surface have been labeled by **1**, this voltammetry can tentatively be attributed to the remaining electroactive *para*-quinone surface groups on the graphite. Thus, by comparing the peak areas of systems I and II with that of system III, we quantified the distribution of *ortho*- and *para*-quinones on the graphite surface (Table 3).

Table 3. Surface Coverage of *ortho*-Quinones on Graphite and GC Powders Determined by Labeling with 1 and the Surface Coverage of *para*-Quinones (Unlabeled) Determined from the Corresponding Voltammetric Peak (System III)

material	surface coverage of *ortho*-quinones (mol cm^{-2})	surface coverage of *para*-quinones (mol cm^{-2})
graphite powder	1.3×10^{-10}	3.4×10^{-11}
GC powder	5.0×10^{-12}	1.7×10^{-11}

By comparison with the labeled graphite powder the voltammetry of the labeled GC powder exhibits only one small set of voltammetric peaks at −0.55 V, which are not observed in unmodified GC and which correspond to the labeling of surface *ortho*-quinones with **1** to form a surface phenazine derivative. In this case the peak corresponding to unlabeled electroactive *para*-quinone groups is both broader and relatively larger than that observed in the graphite powder (Table 3). These results would indicate that, on the graphite powder used herein, *ortho*-quinone groups form the predominant quinone-like surface species, while on the GC powder it is the *para*-quinone groups which are predominant. This is in direct contrast to the previous work of Schreurs et al.[73] discussed in the Introduction; however, in their work the GC electrode was subjected to a pretreatment using radio frequency plasma etching, and as discussed above the distribution and coverage of each type of surface functionality will vary widely from sample to sample even of the same material, depending strongly on the method of manufacture,

(98) Cherezova, E. A.; Taraskina, T. V.; Kulikova, M. V.; Balashev, K. P. *Russ. J. Gen. Chem.* **2003**, *73*, 1160.
(99) Puskas, Z.; Inzelt, G. *Electrochim. Acta* **2005**, *50*, 1481.
(100) Azariah, A. N.; Berchmans, S.; Yegnaraman, V. *Bull. Electrochem.* **1998**, *14*, 309.
(101) Puskas, Z.; Inzelt, G. *J. Solid State Electrochem.* **2004**, *8*, 828.
(102) Komura, T.; Ishihara, M.; Yamaguchi, T.; Takahashi, K. *J. Electroanal. Chem.* **2000**, *493*, 84.
(103) Inzelt, G.; Csahok, E. *Electroanalysis* **1999**, *11*, 744.
(104) Chen, C.; Gao, Y. *Electrochim. Acta* **2007**, *52*, 3143.
(105) Sun, W.; Yang, M.; Jiao, K. *Int. J. Electrochem. Sci.* **2007**, *2*, 93.
(106) Yang, C.; Yi, J.; Tang, X.; Zhou, G.; Zeng, Y. *Reactive Funct. Polymers* **2006**, *66*, 1336.
(107) Heli, H.; Bathaie, S. Z.; Mousavi, M. F. *Electrochim. Acta* **2005**, *51*, 1108.
(108) Johan Foster, E.; Bradley Jones, R.; Laviguer, C.; Williams, V. E. *J. Am. Chem. Soc.* **2006**, *128*, 8569.
(109) Rubenstein, I. *J. Electroanal. Chem.* **1985**, *183*, 379.
(110) Darchen, A.; Moinet, C. *J. Electroanal. Chem.* **1975**, *61*, 373.
(111) Laviron, E.; Meuner-Prest, R.; Lacasse, R. *J. Electroanal. Chem.* **1994**, *375*, 263.
(112) Baeza, A.; Ortiz, J. L.; González, I. *J. Electroanal. Chem.* **1997**, *429*, 121.

pretreatment, storage, history of usage, and so forth. What is clear is that the methods of chemically labeling the target oxygen-containing surface groups of interest, such as *ortho*-quinones, allows us to quantitatively differentiate them and thus form a "surface map" of the species present. The above results were also confirmed by labeling GC, eppg, and bppg electrodes with **1** in a similar fashion, where qualitatively similar results were observed. Again, on the graphite electrodes *ortho*-quinones were predominant over *para*-quinones, while again the opposite was true of the GC electrode.

The labeling of surface *ortho*-quinones on graphite and GC powders with **2** also produced a voltammetric response similar to that discussed above (section 3.3.1) for the nitro derivative of **8**. Again the irreversible six-electron, six-proton reduction of the nitro group could be observed at potentials similar to those expected for system I, while the corresponding oxidation of the arylamine product formed was observed at approximately +0.25 V versus SCE at pH 6.8. On subsequent scans the voltammetric waves associated with the phenazine adduct formed by the action of **2** on the *ortho*-quinone groups could be observed. Again, on the GC powder labeled with **2**, the nitro reduction peak could be observed, but the corresponding voltammetry of system I produced small, poorly resolved peaks, while the system corresponding to the surface *para*-quinones was once again well-defined. The relative amounts of each quinone group present on each type of carbon surface as measured by labeling with **1** is also shown in Table 3 for comparison.

A series of control experiments comparing the solution-phase voltammetry of **1** and **2** reassuringly confirmed that the voltammetry observed in the case of the modified graphite and GC powders was markedly different from that of **1** and **2** in the absence of reaction with surface quinone groups, such as if these compounds were simply physisorbed onto the carbon surface.

Finally a series of control experiments were performed on both the graphite and GC powders involving carrying out the derivatization reaction with one of compounds **3**−**5** replacing the 1,2-phenylenediamine derivatives **1** and **2** used above. Note that phenazine ring formation is not possible with any of these 1,4-substituted compounds.

In the case of labeling with **3**, no voltammetry could be observed in the region of system I, confirming that the voltammetry observed above for the case of labeling with **1** was due to substitution of surface quinone groups by *both* amine groups. However, additional voltammetric waves concurrent with those of system III could be observed corresponding to substitution of single carbonyl groups by one of the amine groups in **3** to form quinimine-like adducts which have redox potentials similar to quinones themselves.[113−116] For both **4** and **5** the corresponding nitro group reduction could be observed, indicating again that formation of the nitro derivative of a quinone-imine adduct was formed on the surface, but again no voltammetry corresponding to system I could be observed.

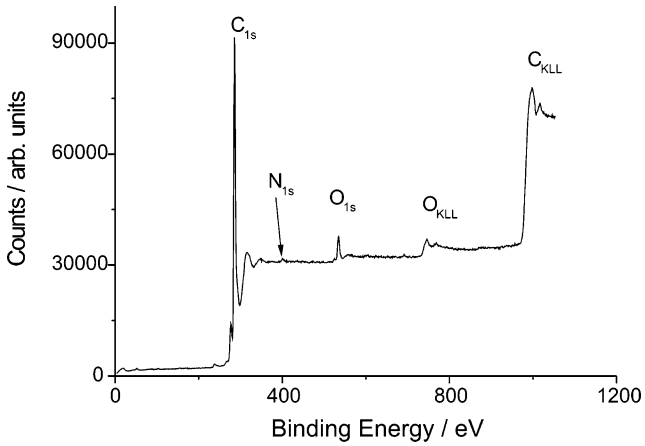

Figure 6. Wide survey XPS spectrum (0−1200 eV) of graphite powder labeled with **1**.

Table 4. Percentage Elemental Surface Composition of Graphite Powder Labeled with 1 and 2 and the Percentage of the Total Oxygen-Containing Groups Attributed to *ortho*-Quinones

labeling compound	% C ± 0.1%	% O ± 0.1%	% N ± 0.1%	percentage of total oxygen attributed to *ortho*-quinones
1	95.8	3.3	0.9	27
2	93.3	5.5	1.2	22

3.3.3. XPS Labeling of Surface ortho-Quinones on the Surface of Graphite Powder. XPS analysis was performed on graphite powder labeled with compounds **1** and **2** to compare with the results of the XPS labeling using the hexamminechromium(III) complex. A wide survey scan was again recorded from 0 to 1200 eV, and the three spectral peaks corresponding to emission from the C(1s), N(1s), and O(1s) levels were observed at 286.5, 400.7, and 534.6 eV, respectively (Figure 6). Table 4 details the percentage elemental surface composition of the two materials. Assuming that the phenylenediamine compounds label *ortho*-quinones only, in a 1:1 ratio the percentage of the total oxygen-containing surface groups corresponding to *ortho*-quinones can be estimated (also shown in Table 4).

4. Conclusions

Ortho- and *para*-quinones on the surface of graphitic carbon electrode materials can be differentiated voltammetrically using CV and/or XPS by labeling them with either the inorganic hexamminechromium(III) complex or organic derivatives of 1,2-phenylenedimaines which form phenazine-like adducts with surface *ortho*-quinones which give rise to a distinct voltammetric signal. In the case of graphite itself the number of *ortho*-quinones was found to be almost four times larger than the number of *para*-quinones. In contrast on the GC surface the number of *ortho*-quinones was significantly smaller than the *para*-quinones, with very few surface functional groups being in the form of *ortho*-quinones on the GC surface. The absolute numbers and relative distribution of the two types of quinone surface species will vary from sample to sample depending on material history, method of manufacture, and pretreatment. This work has shown that we can *chemically* distinguish these different types of surface groups and that, coupled with other chemical

(113) Heras, A. M.; Avila, J. L.; Ruiz, J. J.; Garcia-Blanco, F. *Electrochim. Acta* **1984**, *29*, 541.
(114) Theodoridou, E.; Karabinas, P.; Jannakoudakis, D. *Z. Naturforsch., B* **1982**, *37*, 97.
(115) Bamberger, R. L.; Strohl, J. H. *Anal. Chem.* **1969**, *41*, 1450.
(116) Glicksman, R. *J. Electrochem. Soc.* **1961**, *108*, 1.

methods of labeling the various oxygen-containing functional surface groups developed by us previously, we can begin to develop a "road map" of the number and distributions of surface functionality present on a given graphitic sample.

Acknowledgment. G.G.W. thanks St. John's College, Oxford, for a Junior Research Fellowship.

Supporting Information Available: XPS characterization, ^{1}H NMR characterization of compounds **8** and **9**, and additional voltammetry of graphite electrodes labeled with the hexamminechromium(III) complex (PDF). This material is available free of charge via the Internet at http://pubs.acs.org.

CM071412A